crystallization papers

Crystallization of CcdB in complex with a GyrA fragment

Minh-Hoa Dao-Thi,[a] Laurence Van Melderen,[b] Erwin De Genst,[a] Lieven Buts,[a] An Ranquin,[a] Lode Wyns[a] and Remy Loris[a]*

[a]Laboratorium voor Ultrastructuur, Vlaams Instituut voor Biotechnologie, Vrije Universiteit Brussel, Pleinlaan 2, B-1050 Brussel, Belgium, and [b]Laboratoire de Génétique des Procaryotes, Institut de Biologie et Médecine, Université Libre de Bruxelles, Gosselies, Belgium

Correspondence e-mail: reloris@vub.ac.be

Plasmid addiction systems consist of a plasmid-encoded toxin–antidote pair that serves to stabilize low-copy-number plasmids in bacterial populations. CcdB, the toxin from the *ccd* system on the *Escherichia coli* F plasmid, acts as a gyrase poison. A 14 kDa fragment of gyrase, GyrA14, was found to bind to the toxin CcdB with an affinity of 1.75×10^{-8} *M*. Crystals of the $(GyrA14)_2$ dimer in its free state belong to space group $P4_32_12$, with unit-cell parameters $a = 86.4$, $c = 89.4$ Å, and diffract to 2.4 Å. Crystals of the $(GyrA14)_2$–$(CcdB)_2$ complex belong to space group $P2_12_12_1$, with $a = 52.1$, $b = 83.3$, $c = 110.9$ Å, and diffract to 2.8 Å resolution.

1. Introduction

Maintenance of the F plasmid in *Escherichia coli* cultures is ensured by a number of synergistic processes. The plasmid contains a partitioning system to distribute plasmid copies to the daughter cells during cell division as well as several site-specific recombination systems to resolve oligomeric plasmid molecules. In addition, the F plasmid and other low-copy-number plasmids encode toxin–antidote (TA) systems (reviewed by Engelberg-Kulka & Glaser, 1999). Such TA systems, also called 'plasmid addiction systems', consist of a small operon that contains the genes for a toxic protein and its antidote. In the case of the F plasmid, this operon is called *ccd* (Jaffé *et al.*, 1985) and encodes the antidote CcdA and the toxin CcdB (Miki *et al.*, 1984).

During normal cell growth, both CcdA and CcdB are expressed at low levels. The proteins form a non-covalent complex that acts as a repressor for the transcription of the *ccd* operon (Tam & Kline, 1989; De Feyter *et al.*, 1989). Complex formation also prevents the toxic action of CcdB. Contrary to the stable CcdB, CcdA is a thermodynamically unstable protein (Dao-Thi *et al.*, 2000) that is a substrate for the Lon protease (Van Melderen *et al.*, 1996). Upon accidental plasmid loss CcdA is quickly degraded, activating CcdB (Van Melderen *et al.*, 1994). The interactions between CcdA and CcdB and between the proteins and their operator DNA are complex, do not follow simple stoichiometric binding and are a matter of considerable debate (Dao-Thi *et al.*, 2002; Afif *et al.*, 2001).

The target of CcdB is the *A* subunit of gyrase (Bernard & Couturier, 1992). CcdB traps gyrase during its reaction cycle to form a ternary CcdB–gyrase–DNA complex (Bernard *et al.*, 1993). In this complex, the dsDNA is cleaved, but remains covalently attached to gyrase. This DNA-bound CcdB–gyrase complex is believed to form a barrier to the passage of polymerases, thus blocking transcription (Critchlow *et al.*, 1997).

Crystal structures of two addiction toxins are available, CcdB from the F plasmid (Loris *et al.*, 1999) and Kid from the R1 plasmid (Hargreaves *et al.*, 2002), as well as for the antidote MazE that is part of the *maz* system on the *E. coli* chromosome (Loris *et al.*, 2003). In addition, structures have been presented for the MazE–MazF toxin–antidote complex (Kamada *et al.*, 2003), as well as for the toxin–antidote complex of the unrelated ε–ζ system from *Streptomyces pyogenes* plasmid pSM19035 (Meinhart *et al.*, 2003). No structures of a toxin–target complex are available. Here, we present the crystallization of the dimerization domain of GyrA (residues 363–494 of the *A* chain of gyrase, hereafter called GyrA14) and its complex with CcdB.

2. Cloning, expression and purification

CcdB was prepared as described previously (Dao-Thi *et al.*, 1998). The GyrA14 fragment was amplified by the polymerase chain reaction (PCR) from DNA of plasmid pRJR242, which contains the GyrA64 gene as described in Reece & Maxwell (1991) using the following primers containing the *Bam*HI and *Nde*I sites: GyrA3 *Bam*HI, 5′-CGGGATCCCTAACGA-TCGGCGCTACCAAGAATACG-3′; GyrA4 *Nde*I, 5′-GGAATTCCATATGACCCGTCG-TACTATTTTCGAACTG-3′.

The amplified fragments were then digested by *Nde*I and *Bam*HI and ligated with ligated with plasmid pET15b (containing an N-terminal His$_6$-tag), which had been digested with the same restriction enzymes. The ligated

Table 1
Data-collection statistics.

Values in parentheses are for the last resolution shell.

	GyrA14	GyrA14–CcdB
Beamline	X13 (DESY)	ID14-1 (ESRF)
Resolution (Å)	20.0–2.4 (2.5–2.4)	20.0–2.8
Space group	$P4_32_12$	$P2_12_12_1$
Unit-cell parameters (Å)	$a = b = 86.4$, $c = 89.4$	$a = 52.1$, $b = 83.3$, $c = 110.9$
Completeness (%)	96.5 (99.3)	98.4 (99.9)
$\langle I/\sigma(I) \rangle$	15.3 (3.1)	9.8 (3.4)
No. measured reflections	58396 (6185)	49923 (8477)
No. unique reflections	13295 (1335)	12291 (1498)
No. reflections >3σ	10205 (526)	11455 (1220)
R_{merge}	0.064 (0.410)	0.121 (0.286)

samples were transformed into MC1061 cells to allow selection of GyrA14-harbouring plasmids. These plasmids were then repurified and the nucleotide sequences and orientation of the cloned fragments were checked. Plasmids containing the GyrA14 gene were transformed in BL21 (DE3) pLysS cells for expression.

Cells were grown at 310 K in TB medium until the cell density reached an $OD_{600\,nm}$ of 0.8–1.0. The culture was then induced by adding isopropyl-α-D-thiogalactosidase (IPTG) to a final concentration of 1 mM and incubated overnight at 301 K. Cells were harvested by centrifugation and resuspended in TES (0.2 M Tris, 0.5 mM EDTA and 0.5 M sucrose; 6 ml was used per 300 ml of original culture volume). The protease inhibitors 4-(2-aminoethyl)benzenesulfonyl fluoride (AEBSF) and leupeptine were added and the suspension shaken for 1.5 h on ice. TES/4 (one part TES, three parts H_2O; 9 ml was used per 300 ml of original volume) was then added, followed by further shaking for 1 h. The lysate was centrifuged for 30 min at 14 000 rev min^{-1} at 277 K. The supernatant with soluble proteins was applied to an Ni^{2+}–NTA column, followed by two washing steps: firstly with 50 mM phosphate buffer pH 7.0 and 1 M NaCl and secondly with 50 mM phosphate buffer pH 6.0 and 1 M NaCl. The His-tag proteins were eluted with 50 mM sodium acetate buffer pH 4.5 and neutralized with 1 M Tris buffer pH 8.0. Proteins were concentrated and applied onto a Superdex-75 gel-filtration column (run with 50 mM Tris pH 8.0 plus 150 mM NaCl). This resulted in a protein sample showing only a single band of the correct molecular weight (14 kDa) on SDS–PAGE and yielded about 15 mg GyrA14 per litre of culture.

3. Surface plasmon resonance

GyrA14 (in 10 mM MES pH 5.8) was covalently immobilized on a flow cell of a CM5 sensor chip *via* its surface-exposed lysines to a density of 1.5 µg cm^{-2}. The reference flow cell was coated with a camel single-domain antibody at a density of 1.6 µg cm^{-2}. CcdB-binding data were obtained using a Biacore 3000 instrument at 298 K and 30 µl min^{-1} using PBS (137 mM NaCl, 2.6 mM KCl, 10 mM Na_2HPO_4 and 1.8 mM KH_2PO_4) supplemented with 3 mM EDTA and 0.05% surfactant Tween P20. The CcdB samples were prepared as a concentration series of 0–5000 nM in the same buffer. All binding cycles were performed in duplicate, including the zero-concentration cycle (injection of running buffer). Between each cycle, complete dissociation was obtained by extensive washing with the running buffer. The binding curves were analyzed with the *BIAeval* software and yielded a dissociation rate of 4.85×10^{-4} s^{-1}, an association rate of 2.78×10^4 M^{-1} s^{-1} and a dissociation constant of 1.75×10^{-8} M for a 2:2 binding stoichiometry [one $(CcdB)_2$ dimer binding to one $(GyrA14)_2$ dimer].

4. Crystallization and X-ray diffraction

4.1. GyrA14

Crystallization of $(GyrA14)_2$ was screened by hanging-drop vapour diffusion using the Hampton Research Crystal Screen I and Crystal Screen II kits. Large single crystals of $(GyrA14)_2$ were obtained at 293 K starting from a protein stock solution of 7.0–10.0 mg ml^{-1} (in 50 mM Tris pH 8.0 and 150 mM NaCl) and a reservoir solution consisting of 0.4–0.8 M ammonium phosphate in 100 mM sodium cacodylate buffer pH 6.5 or 100 mM HEPES buffer pH 7.5. 4 µl drops were prepared by mixing 2 µl protein solution with 2 µl precipitant solution.

Bipyramidal crystals of $(GyrA14)_2$ grew to maximum dimensions of $0.15 \times 0.15 \times 0.15$ mm (Fig. 1a). They belong to space group $P4_32_12$, with unit-cell parameters $a = b = 86.4$, $c = 89.4$ Å. Diffraction was observed to 2.4 Å resolution when flash-cooled (using artificial mother liquor with

30% glycerol added as a cryoprotectant) on EMBL beamline X13 at the DESY synchrotron (Hamburg, Germany). A full data set was collected using 0.5° rotations, the statistics of which are shown in Table 1. Data were processed using the *HKL* software (Otwinowski & Minor, 1997). The true enantiomorph of the space group ($P4_32_12$ *versus* $P4_32_12$) was established by performing molecular-replacement calculations with residues 381–475 of the GyrA14 fragment in both space groups (the initial model was taken from the structure of GyrA59; PDB code 1ab4; Morais-Cabral *et al.*, 1997). Using *AMoRe* (Navaza, 1994), only space group $P4_32_12$ gave a clear solution for a single $(GyrA14)_2$ dimer in the asymmetric unit. After preliminary rigid-body refinement using all data to 3.0 Å, the R factor was 0.473 and R_{free} was 0.481.

4.2. GyrA14–CcdB

The $(GyrA14)_2$–$(CcdB)_2$ complex was prepared by mixing the proteins in an approximately 1:1.2 ratio and was purified by gel filtration on a Superdex-75 column. From the elution volume of the complex, it was estimated to be a heterotetramer consisting of a $(CcdB)_2$ dimer and a $(GyrA14)_2$ dimer. Analysis of the purified complex on SDS–PAGE shows two bands of approximately equal intensity, in agreement with a 2:2 stoichiometry (Fig. 2). The dissociation constant of the complex was determined to be 1.75×10^{-8} M by surface plasmon resonance. This is about two magnitudes weaker than the value obtained for the complex formed between $(CcdB)_2$ and the larger $(GyrA59)_2$ fragment (Kampranis *et al.*, 1999). The complex formed appeared to constitute a tetramer. The pure complex was concentrated to 7.0–10.0 mg ml^{-1} in 50 mM Tris–HCl buffer pH 8.0 containing 150 mM NaCl. Under these
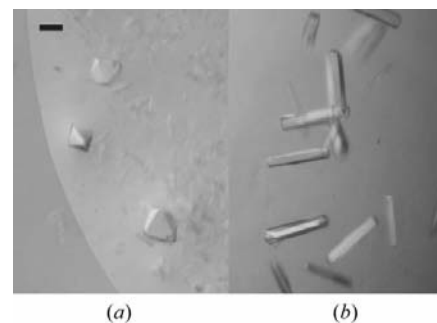

Figure 1
Crystals of $(GyrA14)_2$ and $(GyrA14)_2$–$(CcdB)_2$. The black bar in the top left corner corresponds to 0.1 mm. (*a*) Typical bipyramidal crystals of $(GyrA14)_2$. (*b*) Crystals of the $(GyrA14)_2$–$(CcdB)_2$ complex grown from KCl and PEG 4000.
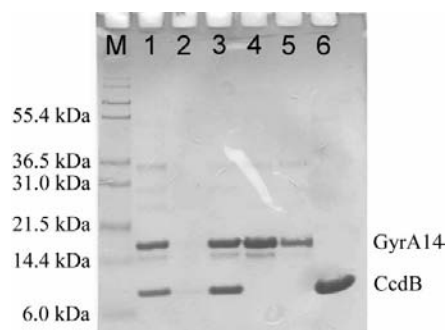
crystallization papers

Figure 2
SDS–polyacrylamide gel (10%) proving the nature of the $(GyrA14)_2$–$(CcdB)_2$ co-crystals. Lane *M*, molecular-weight markers; lane 1, $(GyrA14)_2$–$(CcdB)_2$ redissolved co-crystal; lane 2, washing solution of the dissolved $(GyrA14)_2$–$(CcdB)_2$ co-crystal; lane 3, $(GyrA14)_2$–$(CcdB)_2$ complex purified by gel filtration; lane 4, purified GyrA14; lane 5, redissolved crystal of GyrA14; lane 6, purified CcdB. The weak band just below the GyrA14 band is most likely to result from partial cleavage of the His tag.

conditions, no dissociation was observed even after incubating the protein solution for two weeks at room temperature. Initial screening for crystals of the $(GyrA14)_2$–$(CcdB)_2$ complex produced crystalline aggregates using the same conditions as for the free $(GyrA14)_2$ crystals. Despite intensive attempts towards optimization, these aggregates remained small and did not diffract.

More elaborate screening using all different commercially available Hampton Research crystallization kits as well as the Stura MD1-20 Footprint Screen eventually produced small crystals in different conditions of the Hampton Research Natrix Kit. After optimization of the pH and precipitant concentration, the best crystals were obtained at 293 K in a hanging-drop configuration with 3 μl protein solution and 3 μl well solution containing 0.2 *M* KCl, 10 m*M* CaCl$_2$, 50 m*M* sodium cacodylate pH 6.0 and 10% PEG 4000. These crystals grew to dimensions of $0.25 \times 0.05 \times 0.05$ mm (Fig. 1*b*) and diffracted to 2.8 Å resolution

when tested on beamline ID14-1 at the ESRF synchrotron (Grenoble, France). A full data set was collected, the statistics of which are shown in Table 1. For collection of the data set, the crystal was flash-cooled in a nitrogen stream using 30% glycerol (added to the mother liquor) as cryoprotectant. Data were integrated using *MOSFLM* and scaled with *SCALA* from the *CCP*4 suite of programs (Collaborative Computational Project, Number 4, 1994). The crystals belong to space group $P2_12_12_1$ and contain equal amounts of $(GyrA14)_2$ and $(CcdB)_2$ as judged by SDS–PAGE analysis (Fig. 2). Assuming a heterotetrameric complex of the type $(GyrA14)_2$–$(CcdB)_2$ in the asymmetric unit, a Matthews coefficient of 2.37 Å^3 Da^{-1} can be calculated. A smaller complex of the type GyrA14–CcdB would still give an acceptable (although rather high) Matthews coefficient, but is unlikely given that both CcdB and GyrA14 form dimers in solution and that the molecular weight of the complex in solution as assessed by gel filtration also favours the $(GyrA14)_2$–$(CcdB)_2$ complex.

References

Afif, H., Allali, N., Couturier, M. & Van Melderen, L. (2001). *Mol. Microbiol.* **41**, 73–82.
Bernard, P. & Couturier, M. (1992). *J. Mol. Biol.* **226**, 735–745.
Bernard, P., Kézdy, K. E., Van Melderen, L., Steyaert, J., Wyns, L., Pato, M. L., Higgins, P. N. & Couturier, M. (1993). *J. Mol. Biol.* **234**, 534–541.
Collaborative Computational Project, Number 4 (1994). *Acta Cryst.* D**50**, 760–763.
Critchlow, S. E., O'Dea, M. H., Howells, A. J., Couturier, M., Gellert, M. & Maxwell, A. (1997). *J. Mol. Biol.* **273**, 826–839.
Dao-Thi, M.-H., Charlier, D., Loris, R., Maes, D., Messens, J., Wyns, L. & Backmann, J. (2002). *J. Biol. Chem.* **277**, 3733–3742.
Dao-Thi, M.-H., Messens, J., Wyns, L. & Backmann, J. (2000). *J. Mol. Biol.* **299**, 1373–1386.
Dao-Thi, M.-H., Wyns, L., Poortmans, F., Bahassi, E. M., Couturier, M. & Loris, R. (1998). *Acta Cryst.* D**54**, 975–981.
De Feyter, R., Wallace, C. & Lane, D. (1989). *Mol. Gen. Genet.* **218**, 418–486.
Engelberg-Kulka, H. & Glaser, G. (1999). *Annu. Rev. Microbiol.* **53**, 43–70.
Hargreaves, D., Santos-Sierra, S., Giraldo, R., Sabariegos-Jareno, R., de la Cueva-Méndez, G., Boelens, R., Diaz-Orejas, R. & Rafferty, J. B. (2002). *Structure*, **10**, 1425–1433.
Jaffé, A., Ogura, T. & Higara, S. (1985). *J. Bacteriol.* **163**, 841–849.
Kamada, K., Hanaoka, F. & Burley, S. K. (2003). *Mol. Cell*, **11**, 875–884.
Kampranis, S. C., Howells, A. J. & Maxwell, A. (1999). *J. Mol. Biol.* **293**, 733–744.
Loris, R., Dao-Thi, M.-H., Bahassi, E. M., Van Melderen, L., Poortmans, F., Liddington, R., Couturier, M. & Wyns, L. (1999). *J. Mol. Biol.* **285**, 1667–1677.
Loris, R., Marianovsky, I., Lah, J., Laeremans, T., Engelberg-Kulka, H., Glaser, G., Muyldermans, S. & Wyns, L. (2003). *J. Biol. Chem.* **278**, 28252–28257.
Meinhart, A., Alonso, J. C., Sträter, N. & Saenger, W. (2003). *Proc. Natl Acad. Sci. USA*, **100**, 1661–1666.
Miki, T., Chang, Z.-T & Horiuchi, T. (1984). *J. Mol. Biol.* **174**, 627–646.
Morais-Cabral, J. H., Jackson, A. P., Smith, C. V., Shikotra, N., Maxwell, A. & Liddington, R. C. (1997). *Nature (London)*, **388**, 903–906.
Navaza, J. (1994). *Acta Cryst.* A**50**, 157–163.
Otwinowski, Z. & Minor, W. (1997). *Methods Enzymol.* **276**, 307–326.
Reece, R. J. & Maxwell, A. (1991). *J. Biol. Chem.* **266**, 3540–3546.
Tam, J. E. & Kline, B. C. (1989). *Mol. Gen. Genet.* **219**, 26–32.
Van Melderen, L., Bernard, P. & Couturier, M. (1994). *Mol. Microbiol.* **11**, 1151–1157.
Van Melderen, L., Dao-Thi, M.-H., Lecchi, P., Gottesman, S., Couturier, M. & Maurizi, M. R. (1996). *J. Biol. Chem.* **271**, 27730–27738.